Title

Observation of new resonances decaying to Dπ and D*π in inclusive e+e- collisions near s=10.58 GeV

Journal

Physical Review D, 82(11)

ISSN

2470-0010

Authors

del Amo Sanchez, P
Lees, JP
Poireau, V
et al.

Publication Date

2010-12-01

DOI

10.1103/physrevd.82.111101

RAPID COMMUNICATIONS

PHYSICAL REVIEW D **82,** 111101(R) (2010)

Observation of new resonances decaying to $D\pi$ and $D^*\pi$ in inclusive e^+e^- collisions near $\sqrt{s} = 10.58$ GeV

P. del Amo Sanchez,[1] J. P. Lees,[1] V. Poireau,[1] E. Prencipe,[1] V. Tisserand,[1] J. Garra Tico,[2] E. Grauges,[2] M. Martinelli,[3a,3b] A. Palano,[3a,3b] M. Pappagallo,[3a,3b] G. Eigen,[4] B. Stugu,[4] L. Sun,[4] M. Battaglia,[5] D. N. Brown,[5] B. Hooberman,[5] L. T. Kerth,[5] Yu. G. Kolomensky,[5] G. Lynch,[5] I. L. Osipenkov,[5] T. Tanabe,[5] C. M. Hawkes,[6] A. T. Watson,[6] H. Koch,[7] T. Schroeder,[7] D. J. Asgeirsson,[8] C. Hearty,[8] T. S. Mattison,[8] J. A. McKenna,[8] A. Khan,[9] A. Randle-Conde,[9] V. E. Blinov,[10] A. R. Buzykaev,[10] V. P. Druzhinin,[10] V. B. Golubev,[10] A. P. Onuchin,[10] S. I. Serednyakov,[10] Yu. I. Skovpen,[10] E. P. Solodov,[10] K. Yu. Todyshev,[10] A. N. Yushkov,[10] M. Bondioli,[11] S. Curry,[11] D. Kirkby,[11] A. J. Lankford,[11] M. Mandelkern,[11] E. C. Martin,[11] D. P. Stoker,[11] H. Atmacan,[12] J. W. Gary,[12] F. Liu,[12] O. Long,[12] G. M. Vitug,[12] C. Campagnari,[13] T. M. Hong,[13] D. Kovalskyi,[13] J. D. Richman,[13] C. West,[13] A. M. Eisner,[14] C. A. Heusch,[14] J. Kroseberg,[14] W. S. Lockman,[14] A. J. Martinez,[14] T. Schalk,[14] B. A. Schumm,[14] A. Seiden,[14] L. O. Winstrom,[14] C. H. Cheng,[15] D. A. Doll,[15] B. Echenard,[15] D. G. Hitlin,[15] P. Ongmongkolkul,[15] F. C. Porter,[15] A. Y. Rakitin,[15] R. Andreassen,[16] M. S. Dubrovin,[16] G. Mancinelli,[16] B. T. Meadows,[16] M. D. Sokoloff,[16] P. C. Bloom,[17] W. T. Ford,[17] A. Gaz,[17] M. Nagel,[17] U. Nauenberg,[17] J. G. Smith,[17] S. R. Wagner,[17] R. Ayad,[18,*] W. H. Toki,[18] H. Jasper,[19] T. M. Karbach,[19] J. Merkel,[19] A. Petzold,[19] B. Spaan,[19] K. Wacker,[19] M. J. Kobel,[20] K. R. Schubert,[20] R. Schwierz,[20] D. Bernard,[21] M. Verderi,[21] P. J. Clark,[22] S. Playfer,[22] J. E. Watson,[22] M. Andreotti,[23a,23b] D. Bettoni,[23a] C. Bozzi,[23a] R. Calabrese,[23a,23b] A. Cecchi,[23a,23b] G. Cibinetto,[23a,23b] E. Fioravanti,[23a,23b] P. Franchini,[23a,23b] E. Luppi,[23a,23b] M. Munerato,[23a,23b] M. Negrini,[23a,23b] A. Petrella,[23a,23b] L. Piemontese,[23a] R. Baldini-Ferroli,[24] A. Calcaterra,[24] R. de Sangro,[24] G. Finocchiaro,[24] M. Nicolaci,[24] S. Pacetti,[24] P. Patteri,[24] I. M. Peruzzi,[24,†] M. Piccolo,[24] M. Rama,[24] A. Zallo,[24] R. Contri,[25a,25b] E. Guido,[25a,25b] M. Lo Vetere,[25a,25b] M. R. Monge,[25a,25b] S. Passaggio,[25a] C. Patrignani,[25a,25b] E. Robutti,[25a] S. Tosi,[25a,25b] B. Bhuyan,[26] V. Prasad,[26] C. L. Lee,[27] M. Morii,[27] A. Adametz,[28] J. Marks,[28] U. Uwer,[28] F. U. Bernlochner,[29] M. Ebert,[29] H. M. Lacker,[29] T. Lueck,[29] A. Volk,[29] P. D. Dauncey,[30] M. Tibbetts,[30] P. K. Behera,[31] U. Mallik,[31] C. Chen,[32] J. Cochran,[32] H. B. Crawley,[32] L. Dong,[32] W. T. Meyer,[32] S. Prell,[32] E. I. Rosenberg,[32] A. E. Rubin,[32] A. V. Gritsan,[33] Z. J. Guo,[33] N. Arnaud,[34] M. Davier,[34] D. Derkach,[34] J. Firmino da Costa,[34] G. Grosdidier,[34] F. Le Diberder,[34] A. M. Lutz,[34] B. Malaescu,[34] A. Perez,[34] P. Roudeau,[34] M. H. Schune,[34] J. Serrano,[34] V. Sordini,[34,‡] A. Stocchi,[34] L. Wang,[34] G. Wormser,[34] D. J. Lange,[35] D. M. Wright,[35] I. Bingham,[36] C. A. Chavez,[36] J. P. Coleman,[36] J. R. Fry,[36] E. Gabathuler,[36] R. Gamet,[36] D. E. Hutchcroft,[36] D. J. Payne,[36] C. Touramanis,[36] A. J. Bevan,[37] F. Di Lodovico,[37] R. Sacco,[37] M. Sigamani,[37] G. Cowan,[38] S. Paramesvaran,[38] A. C. Wren,[38] D. N. Brown,[39] C. L. Davis,[39] A. G. Denig,[40] M. Fritsch,[40] W. Gradl,[40] A. Hafner,[40] K. E. Alwyn,[41] D. Bailey,[41] R. J. Barlow,[41] G. Jackson,[41] G. D. Lafferty,[41] J. Anderson,[42] R. Cenci,[42] A. Jawahery,[42] D. A. Roberts,[42] G. Simi,[42] J. M. Tuggle,[42] C. Dallapiccola,[43] E. Salvati,[43] R. Cowan,[44] D. Dujmic,[44] G. Sciolla,[44] M. Zhao,[44] D. Lindemann,[45] P. M. Patel,[45] S. H. Robertson,[45] M. Schram,[45] P. Biassoni,[46a,46b] A. Lazzaro,[46a,46b] V. Lombardo,[46a] F. Palombo,[46a,46b] S. Stracka,[46a,46b] L. Cremaldi,[47] R. Godang,[47,§] R. Kroeger,[47] P. Sonnek,[47] D. J. Summers,[47] X. Nguyen,[48] M. Simard,[48] P. Taras,[48] G. De Nardo,[49a,49b] D. Monorchio,[49a,49b] G. Onorato,[49a,49b] C. Sciacca,[49a,49b] G. Raven,[50] H. L. Snoek,[50] C. P. Jessop,[51] K. J. Knoepfel,[51] J. M. LoSecco,[51] W. F. Wang,[51] L. A. Corwin,[52] K. Honscheid,[52] R. Kass,[52] J. P. Morris,[52] N. L. Blount,[53] J. Brau,[53] R. Frey,[53] O. Igonkina,[53] J. A. Kolb,[53] R. Rahmat,[53] N. B. Sinev,[53] D. Strom,[53] J. Strube,[53] E. Torrence,[53] G. Castelli,[54a,54b] E. Feltresi,[54a,54b] N. Gagliardi,[54a,54b] M. Margoni,[54a,54b] M. Morandin,[54a] M. Posocco,[54a] M. Rotondo,[54a] F. Simonetto,[54a,54b] R. Stroili,[54a,54b] E. Ben-Haim,[55] G. R. Bonneaud,[55] H. Briand,[55] G. Calderini,[55] J. Chauveau,[55] O. Hamon,[55] Ph. Leruste,[55] G. Marchiori,[55] J. Ocariz,[55] J. Prendki,[55] S. Sitt,[55] M. Biasini,[56a,56b] E. Manoni,[56a,56b] A. Rossi,[56a,56b] C. Angelini,[57a,57b] G. Batignani,[57a,57b] S. Bettarini,[57a,57b] M. Carpinelli,[57a,57b,∥] G. Casarosa,[57a,57b] A. Cervelli,[57a,57b] F. Forti,[57a,57b] M. A. Giorgi,[57a,57b] A. Lusiani,[57a,57c] N. Neri,[57a,57b] E. Paoloni,[57a,57b] G. Rizzo,[57a,57b] J. J. Walsh,[57a] D. Lopes Pegna,[58] C. Lu,[58] J. Olsen,[58] A. J. S. Smith,[58] A. V. Telnov,[58] F. Anulli,[59a] E. Baracchini,[59a,59b] G. Cavoto,[59a] R. Faccini,[59a,59b] F. Ferrarotto,[59a] F. Ferroni,[59a,59b] M. Gaspero,[59a,59b] L. Li Gioi,[59a] M. A. Mazzoni,[59a] G. Piredda,[59a] F. Renga,[59a,59b] T. Hartmann,[60] T. Leddig,[60] H. Schröder,[60] R. Waldi,[60] T. Adye,[61] B. Franek,[61] E. O. Olaiya,[61] F. F. Wilson,[61] S. Emery,[62] G. Hamel de Monchenault,[62] G. Vasseur,[62] Ch. Yèche,[62] M. Zito,[62] M. T. Allen,[63] D. Aston,[63] D. J. Bard,[63] R. Bartoldus,[63] J. F. Benitez,[63] C. Cartaro,[63] M. R. Convery,[63] J. Dorfan,[63] G. P. Dubois-Felsmann,[63] W. Dunwoodie,[63] R. C. Field,[63] M. Franco Sevilla,[63] B. G. Fulsom,[63] A. M. Gabareen,[63] M. T. Graham,[63] P. Grenier,[63] C. Hast,[63] W. R. Innes,[63] M. H. Kelsey,[63] H. Kim,[63] P. Kim,[63] M. L. Kocian,[63] D. W. G. S. Leith,[63] S. Li,[63] B. Lindquist,[63] S. Luitz,[63] V. Luth,[63] H. L. Lynch,[63] D. B. MacFarlane,[63] H. Marsiske,[63] D. R. Muller,[63] H. Neal,[63] S. Nelson,[63] C. P. O'Grady,[63] I. Ofte,[63] M. Perl,[63] T. Pulliam,[63] B. N. Ratcliff,[63] A. Roodman,[63]

1550-7998/2010/82(11)/111101(9)

A. A. Salnikov,[63] V. Santoro,[63] R. H. Schindler,[63] J. Schwiening,[63] A. Snyder,[63] D. Su,[63] M. K. Sullivan,[63] S. Sun,[63] K. Suzuki,[63] J. M. Thompson,[63] J. Va'vra,[63] A. P. Wagner,[63] M. Weaver,[63] C. A. West,[63] W. J. Wisniewski,[63] M. Wittgen,[63] D. H. Wright,[63] H. W. Wulsin,[63] A. K. Yarritu,[63] C. C. Young,[63] V. Ziegler,[63] X. R. Chen,[64] W. Park,[64] M. V. Purohit,[64] R. M. White,[64] J. R. Wilson,[64] S. J. Sekula,[65] M. Bellis,[66] P. R. Burchat,[66] A. J. Edwards,[66] T. S. Miyashita,[66] S. Ahmed,[67] M. S. Alam,[67] J. A. Ernst,[67] B. Pan,[67] M. A. Saeed,[67] S. B. Zain,[67] N. Guttman,[68] A. Soffer,[68] P. Lund,[69] S. M. Spanier,[69] R. Eckmann,[70] J. L. Ritchie,[70] A. M. Ruland,[70] C. J. Schilling,[70] R. F. Schwitters,[70] B. C. Wray,[70] J. M. Izen,[71] X. C. Lou,[71] F. Bianchi,[72a,72b] D. Gamba,[72a,72b] M. Pelliccioni,[72a,72b] M. Bomben,[73a,73b] L. Lanceri,[73a,73b] L. Vitale,[73a,73b] N. Lopez-March,[74] F. Martinez-Vidal,[74] D. A. Milanes,[74] A. Oyanguren,[74] J. Albert,[75] Sw. Banerjee,[75] H. H. F. Choi,[75] K. Hamano,[75] G. J. King,[75] R. Kowalewski,[75] M. J. Lewczuk,[75] I. M. Nugent,[75] J. M. Roney,[75] R. J. Sobie,[75] T. J. Gershon,[76] P. F. Harrison,[76] T. E. Latham,[76] E. M. T. Puccio,[76] H. R. Band,[77] S. Dasu,[77] K. T. Flood,[77] Y. Pan,[77] R. Prepost,[77] C. O. Vuosalo,[77] and S. L. Wu[77]

(*BaBar* Collaboration)

[1]*Laboratoire d'Annecy-le-Vieux de Physique des Particules (LAPP), Université de Savoie, CNRS/IN2P3, F-74941 Annecy-Le-Vieux, France*
[2]*Universitat de Barcelona, Facultat de Fisica, Departament ECM, E-08028 Barcelona, Spain*
[3a]*INFN Sezione di Bari, I-70126 Bari, Italy*
[3b]*Dipartimento di Fisica, Università di Bari, I-70126 Bari, Italy*
[4]*University of Bergen, Institute of Physics, N-5007 Bergen, Norway*
[5]*Lawrence Berkeley National Laboratory and University of California, Berkeley, California 94720, USA*
[6]*University of Birmingham, Birmingham, B15 2TT, United Kingdom*
[7]*Ruhr Universität Bochum, Institut für Experimentalphysik 1, D-44780 Bochum, Germany*
[8]*University of British Columbia, Vancouver, British Columbia, Canada V6T 1Z1*
[9]*Brunel University, Uxbridge, Middlesex UB8 3PH, United Kingdom*
[10]*Budker Institute of Nuclear Physics, Novosibirsk 630090, Russia*
[11]*University of California at Irvine, Irvine, California 92697, USA*
[12]*University of California at Riverside, Riverside, California 92521, USA*
[13]*University of California at Santa Barbara, Santa Barbara, California 93106, USA*
[14]*University of California at Santa Cruz, Institute for Particle Physics, Santa Cruz, California 95064, USA*
[15]*California Institute of Technology, Pasadena, California 91125, USA*
[16]*University of Cincinnati, Cincinnati, Ohio 45221, USA*
[17]*University of Colorado, Boulder, Colorado 80309, USA*
[18]*Colorado State University, Fort Collins, Colorado 80523, USA*
[19]*Technische Universität Dortmund, Fakultät Physik, D-44221 Dortmund, Germany*
[20]*Technische Universität Dresden, Institut für Kern- und Teilchenphysik, D-01062 Dresden, Germany*
[21]*Laboratoire Leprince-Ringuet, CNRS/IN2P3, Ecole Polytechnique, F-91128 Palaiseau, France*
[22]*University of Edinburgh, Edinburgh EH9 3JZ, United Kingdom*
[23a]*INFN Sezione di Ferrara, I-44100 Ferrara, Italy*
[23b]*Dipartimento di Fisica, Università di Ferrara, I-44100 Ferrara, Italy*
[24]*INFN Laboratori Nazionali di Frascati, I-00044 Frascati, Italy*
[25a]*INFN Sezione di Genova, I-16146 Genova, Italy*
[25b]*Dipartimento di Fisica, Università di Genova, I-16146 Genova, Italy*
[26]*Indian Institute of Technology Guwahati, Guwahati, Assam, 781 039, India*
[27]*Harvard University, Cambridge, Massachusetts 02138, USA*
[28]*Universität Heidelberg, Physikalisches Institut, Philosophenweg 12, D-69120 Heidelberg, Germany*
[29]*Humboldt-Universität zu Berlin, Institut für Physik, Newtonstr. 15, D-12489 Berlin, Germany*
[30]*Imperial College London, London, SW7 2AZ, United Kingdom*
[31]*University of Iowa, Iowa City, Iowa 52242, USA*
[32]*Iowa State University, Ames, Iowa 50011-3160, USA*
[33]*Johns Hopkins University, Baltimore, Maryland 21218, USA*
[34]*Laboratoire de l'Accélérateur Linéaire, IN2P3/CNRS et Université Paris-Sud 11, Centre Scientifique d'Orsay, B. P. 34, F-91898 Orsay Cedex, France*
[35]*Lawrence Livermore National Laboratory, Livermore, California 94550, USA*
[36]*University of Liverpool, Liverpool L69 7ZE, United Kingdom*
[37]*Queen Mary, University of London, London, E1 4NS, United Kingdom*
[38]*University of London, Royal Holloway and Bedford New College, Egham, Surrey TW20 0EX, United Kingdom*

[39]*University of Louisville, Louisville, Kentucky 40292, USA*
[40]*Johannes Gutenberg-Universität Mainz, Institut für Kernphysik, D-55099 Mainz, Germany*
[41]*University of Manchester, Manchester M13 9PL, United Kingdom*
[42]*University of Maryland, College Park, Maryland 20742, USA*
[43]*University of Massachusetts, Amherst, Massachusetts 01003, USA*
[44]*Massachusetts Institute of Technology, Laboratory for Nuclear Science, Cambridge, Massachusetts 02139, USA*
[45]*McGill University, Montréal, Québec, Canada H3A 2T8*
[46a]*INFN Sezione di Milano, I-20133 Milano, Italy*
[46b]*Dipartimento di Fisica, Università di Milano, I-20133 Milano, Italy*
[47]*University of Mississippi, University, Mississippi 38677, USA*
[48]*Université de Montréal, Physique des Particules, Montréal, Québec, Canada H3C 3J7*
[49a]*INFN Sezione di Napoli, I-80126 Napoli, Italy*
[49b]*Dipartimento di Scienze Fisiche, Università di Napoli Federico II, I-80126 Napoli, Italy*
[50]*NIKHEF, National Institute for Nuclear Physics and High Energy Physics, NL-1009 DB Amsterdam, The Netherlands*
[51]*University of Notre Dame, Notre Dame, Indiana 46556, USA*
[52]*Ohio State University, Columbus, Ohio 43210, USA*
[53]*University of Oregon, Eugene, Oregon 97403, USA*
[54a]*INFN Sezione di Padova, I-35131 Padova, Italy*
[54b]*Dipartimento di Fisica, Università di Padova, I-35131 Padova, Italy*
[55]*Laboratoire de Physique Nucléaire et de Hautes Energies, IN2P3/CNRS, Université Pierre et Marie Curie-Paris6,*
Université Denis Diderot-Paris7, F-75252 Paris, France
[56a]*INFN Sezione di Perugia, I-06100 Perugia, Italy*
[56b]*Dipartimento di Fisica, Università di Perugia, I-06100 Perugia, Italy*
[57a]*INFN Sezione di Pisa, I-56127 Pisa, Italy*
[57b]*Dipartimento di Fisica, Università di Pisa, I-56127 Pisa, Italy*
[57c]*Scuola Normale Superiore di Pisa, I-56127 Pisa, Italy*
[58]*Princeton University, Princeton, New Jersey 08544, USA*
[59a]*INFN Sezione di Roma, I-00185 Roma, Italy*
[59b]*Dipartimento di Fisica, Università di Roma La Sapienza, I-00185 Roma, Italy*
[60]*Universität Rostock, D-18051 Rostock, Germany*
[61]*Rutherford Appleton Laboratory, Chilton, Didcot, Oxon, OX11 0QX, United Kingdom*
[62]*CEA, Irfu, SPP, Centre de Saclay, F-91191 Gif-sur-Yvette, France*
[63]*SLAC National Accelerator Laboratory, Stanford, California 94309 USA*
[64]*University of South Carolina, Columbia, South Carolina 29208, USA*
[65]*Southern Methodist University, Dallas, Texas 75275, USA*
[66]*Stanford University, Stanford, California 94305-4060, USA*
[67]*State University of New York, Albany, New York 12222, USA*
[68]*Tel Aviv University, School of Physics and Astronomy, Tel Aviv, 69978, Israel*
[69]*University of Tennessee, Knoxville, Tennessee 37996, USA*
[70]*University of Texas at Austin, Austin, Texas 78712, USA*
[71]*University of Texas at Dallas, Richardson, Texas 75083, USA*
[72a]*INFN Sezione di Torino, I-10125 Torino, Italy*
[72b]*Dipartimento di Fisica Sperimentale, Università di Torino, I-10125 Torino, Italy*
[73a]*INFN Sezione di Trieste, I-34127 Trieste, Italy*
[73b]*Dipartimento di Fisica, Università di Trieste, I-34127 Trieste, Italy*
[74]*IFIC, Universitat de Valencia-CSIC, E-46071 Valencia, Spain*
[75]*University of Victoria, Victoria, British Columbia, Canada V8W 3P6*
[76]*Department of Physics, University of Warwick, Coventry CV4 7AL, United Kingdom*
[77]*University of Wisconsin, Madison, Wisconsin 53706, USA*

(Received 12 September 2010; published 1 December 2010)

We present a study of the $D^+\pi^-$, $D^0\pi^+$, and $D^{*+}\pi^-$ systems in inclusive $e^+e^- \rightarrow c\bar{c}$ interactions in a search for new excited D meson states. We use a data set, consisting of $\sim$454 fb^{-1}, collected at center-of-mass energies near 10.58 GeV by the *BABAR* detector at the SLAC PEP-II asymmetric-energy collider. We

---

[*] Now at Temple University, Philadelphia, PA 19122, USA
[†] Also with Università di Perugia, Dipartimento di Fisica, Perugia, Italy
[‡] Also with Università di Roma La Sapienza, I-00185 Roma, Italy
[§] Now at University of South AL, Mobile, AL 36688, USA
[‖] Also with Università di Sassari, Sassari, Italy

observe, for the first time, candidates for the radial excitations of the D^0, D^{*0}, and D^{*+}, as well as the $L = 2$ excited states of the D^0 and D^+, where L is the orbital angular momentum of the quarks.

DOI: 10.1103/PhysRevD.82.111101 PACS numbers: 14.40.Lb, 12.38.−t, 13.25.Ft

The spectrum of mesons consisting of a charm and an up or a down quark is poorly known. The spectrum of quark-antiquark systems was predicted in 1985 using a relativistic chromodynamic potential model [1]. The low-mass spectrum of the $c\bar{u}$ or $c\bar{d}$ system is comprised of the ground states (1S), the orbital excitations with angular momentum $L = 1, 2$ (1P, 1D), and the first radial excitations (2S). In this paper we label the states using the notation $D_J^{(2S+1)}(nL)$, where J is the total angular momentum of the state, n is the radial quantum number, and L and S are the orbital angular momentum and total spin of the quarks. Besides the ground states (D, D^*), only two 1P states, known as the $D_1(2420)$ and $D_2^*(2460)$ [2], are well-established experimentally since they have relatively narrow widths (~ 30 MeV). In contrast, the other two 1P states, known as the $D_0^*(2400)$ and $D_1'(2430)$, are very broad (~ 300 MeV), making them difficult to detect [3–5].

To search for states not yet observed, we analyze the *inclusive* production of the $D^+\pi^-$, $D^0\pi^+$, and $D^{*+}\pi^-$ [6] final states in the reaction $e^+e^- \rightarrow c\bar{c} \rightarrow D^{(*)}\pi X$, where X is any additional system. We use an event sample consisting of approximately 590×10^6 $e^+e^- \rightarrow c\bar{c}$ events (454 fb^{-1}) produced at e^+e^- center-of-mass (CM) energies near 10.58 GeV and collected with the *BABAR* detector at the SLAC PEP-II asymmetric-energy collider. Our signal yield for the $L = 1$ resonances is more than 10 times larger than the best previous study [7], resulting in much greater sensitivity to higher resonances.

The *BABAR* detector is described in detail in Ref. [8]. Charged-particle momenta are measured with a five-layer, double-sided silicon vertex tracker (SVT) and a 40-layer drift chamber (DCH) inside a 1.5-T superconducting solenoidal magnet. A calorimeter consisting of 6580 CsI(Tl) crystals is used to measure electromagnetic energy. A ring-imaging Cherenkov radiation detector (DIRC), aided by measurements of ionization energy loss, dE/dx, in the SVT and DCH, is used for particle identification (PID) of charged hadrons.

The $D\pi$ system is reconstructed in the neutral $D^+\pi^-$ and charged $D^0\pi^+$ modes, where $D^+ \rightarrow K^-\pi^+\pi^+$ and $D^0 \rightarrow K^-\pi^+$. A PID algorithm is applied to all tracks. Charged kaon identification has an average efficiency of 90% within the acceptance of the detector and an average pion-to-kaon misidentification probability of 1.5%.

For all channels we perform a vertex fit for the D^+ and D^0 daughters. To improve the signal-to-background ratio for $D^+ \rightarrow K^-\pi^+\pi^+$, we require that the measured flight distance of the D^+ candidate from the e^+e^- interaction region be greater than 5 times its uncertainty. To improve the signal purity for $D^0 \rightarrow K^-\pi^+$ we require $\cos\theta_K > -0.9$, where θ_K is the angle formed by the K^- in the D^0 candidate rest frame with respect to the prior direction of the D^0 candidate in the CM reference frame. The $D\pi$ candidates for both D^+ and D^0 are then reconstructed by performing a vertex fit with an additional charged *primary* pion, which originates from the e^+e^- interaction region. For all vertex fits we require a χ^2 probability $>$0.1%.

In the $D^0\pi^+$ sample, we veto D^0 candidates from D^{*+} or D^{*0} decays by forming $D^0\pi^+$ (where the π^+ is any additional pion in the event) and $D^0\pi^0$ combinations, and rejecting the event if the invariant-mass difference between this combination and the D^0 candidate is within 2σ of the nominal D^*-D mass difference [2], where σ is the detector resolution.

The $K^-\pi^+\pi^+$ and $K^-\pi^+$ mass distributions are shown in Figs. 1(a) and 1(b). We fit these distributions to a linear background and a Gaussian signal; the signal widths obtained are $\sigma_{D^+} = 6.7\ \text{MeV}/c^2$ and $\sigma_{D^0} = 7.6\ \text{MeV}/c^2$. The signal region is defined to be within $\pm 2.5\sigma$ of the peak, while sideband regions are defined as the ranges $(\pm 5.0\sigma, \pm 7.5\sigma)$ and $(\pm 4.0\sigma, \pm 6.5\sigma)$ for the D^+ and D^0, respectively. The D^+ signal region has purity $N_S/(N_S + N_B) = 65\%$, where N_S (N_B) is the number of signal (background) events, while the D^0 purity is 83%.

The $D^{*+}\pi^-$ system is reconstructed using the $D^0 \rightarrow K^-\pi^+$ and $D^0 \rightarrow K^-\pi^+\pi^-\pi^+$ decay modes. A D^0

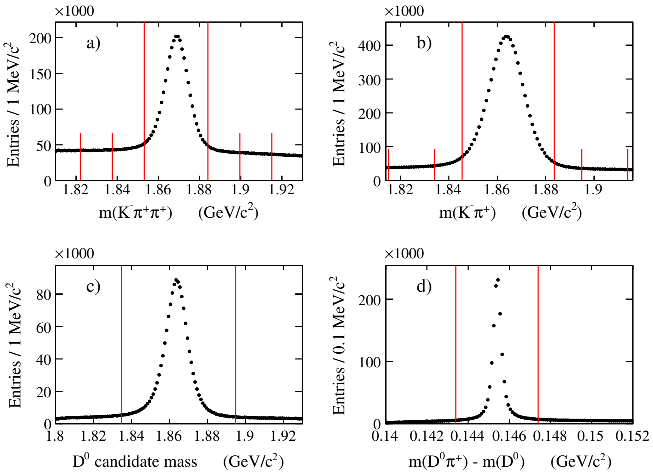

FIG. 1 (color online). Mass distribution for (a) D^+ and (b) D^0 candidates in the $D^+\pi^-$ and $D^0\pi^+$ samples. Plots (c) and (d) correspond to the $D^{*+}\pi^-$ sample and show the mass distribution for D^0 candidates and the Δm distribution for D^{*+} candidates. The vertical lines show the signal and, in (a) and (b), the sideband regions.

candidate is accepted if its invariant mass is within $30\ \mathrm{MeV}/c^2$ of the mean value. A D^{*+} candidate is reconstructed by requiring an additional slow pion (π_s^+) originating from the e^+e^- interaction region. We select a D^{*+} candidate if the mass difference $\Delta m = m(K^-\pi^+(\pi^+\pi^-)\pi_s^+) - m(K^-\pi^+(\pi^+\pi^-))$ is within $2.0\ \mathrm{MeV}/c^2$ of the mean value. The D^0 candidate invariant-mass distribution and the Δm distribution are shown in Figs. 1(c) and 1(d). The D^{*+} signal purity is 89%. Finally, we reconstruct a $D^{*+}\pi^-$ candidate by combining a D^{*+} candidate with an additional charged track identified as a π^- and applying a vertex fit.

Background from $e^+e^- \to B\bar{B}$ events, and much of the combinatorial background, are removed by requiring the CM momentum of the $D^{(*)}\pi$ system to be greater than $3.0\ \mathrm{GeV}/c$. In addition, we remove fake primary pion candidates originating mainly from the opposite side of the event by requiring $\cos\theta_\pi > -0.8$. The angle θ_π is defined in the $D^{(*)}\pi$ rest frame as the angle between the primary pion direction and the prior direction of the $D^{(*)}\pi$ system in the CM frame.

To extract the resonance parameters we define the variables $M(D^+\pi^-) = m(K^-\pi^+\pi^+\pi^-) - m(K^-\pi^+\pi^+) + m_{D^+}$ and $M(D^0\pi^+) = m(K^-\pi^+\pi^+) - m(K^-\pi^+) + m_{D^0}$, where m_{D^+} and m_{D^0} are the values of the D^+ and D^0 mass [2]. The use of the mass difference improves the resolution on the reconstructed mass to about $3\ \mathrm{MeV}/c^2$. We remove the contribution due to fake D^+ and D^0 candidates by subtracting the $M(D\pi)$ distributions obtained by selecting events in the D^+ or D^0 candidate mass sidebands.

The $D^+\pi^-$ and $D^0\pi^+$ mass spectra are presented in Fig. 2 and show similar features.

(i) Prominent peaks for $D_2^*(2460)^0$ and $D_2^*(2460)^+$.

(ii) The $D^+\pi^-$ mass spectrum shows a peaking background (feeddown) at about $2.3\ \mathrm{GeV}/c^2$ due to decays from the $D_1(2420)^0$ and $D_2^*(2460)^0$ to $D^{*+}\pi^-$. The D^{*+} in these events decays to $D^+\pi^0$ and the π^0 is missing in the reconstruction. The missing π^0 has very low momentum because the D^{*+} decay is very close to threshold. Therefore, these decays have a mass resolution of only $5.8\ \mathrm{MeV}/c^2$ and a bias of $-143.2\ \mathrm{MeV}/c^2$. Similarly, $D^0\pi^+$ shows peaking backgrounds due to the decays of the $D_1(2420)^+$ and $D_2^*(2460)^+$ to $D^{*0}\pi^+$, where the D^{*0} decays to $D^0\pi^0$.

(iii) Both $D^+\pi^-$ and $D^0\pi^+$ mass distributions show new structures around 2.6 and $2.75\ \mathrm{GeV}/c^2$. We call these enhancements $D^*(2600)$ and $D^*(2760)$.

We have compared these mass spectra with those obtained from generic $e^+e^- \to \bar{c}c$ Monte Carlo (MC) events. These events were generated using JETSET [9] with all the known particle resonances incorporated. The events are then reconstructed using a detailed GEANT4 [10] detector simulation and the event selection procedure used for the data. In addition, we study $D\pi$ mass spectra from the D^+ and D^0 candidate mass sidebands, as well as mass spectra for wrong-sign $D^+\pi^+$ and $D^0\pi^-$ samples. We find no backgrounds or reflections that can cause the structures at 2.6 and $2.76\ \mathrm{GeV}/c^2$. In the study of the $D^0\pi^+$ final state we find a peaking background due to events where the D^0 candidate is not a true D^0, but the K^- candidate and the primary π^+ candidate are from a true $D^0 \to K^-\pi^+$ decay. These combinations produce enhancements in $M(D^0\pi^+)$ both in the D^0 candidate mass signal region and sidebands. However, we find this background to be linear as a function of the D^0 candidate mass, and it is removed by the sideband subtraction.

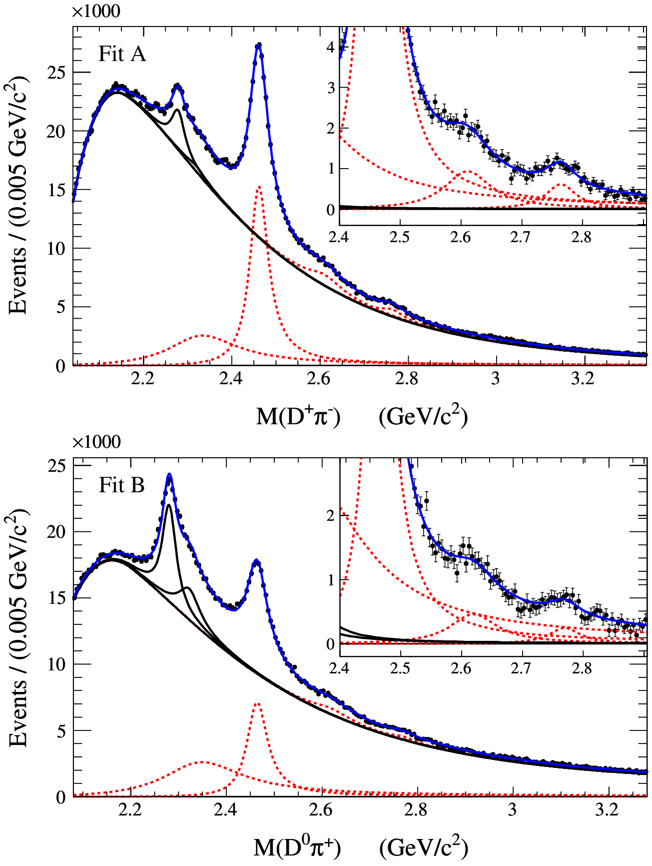

FIG. 2 (color online). Mass distribution for $D^+\pi^-$ (top) and $D^0\pi^+$ (bottom) candidates. Points correspond to data, with the total fit overlaid as a solid curve. The dotted curves are the signal components. The lower solid curves correspond to the smooth combinatoric background and to the peaking backgrounds at $2.3\ \mathrm{GeV}/c^2$. The inset plots show the distributions after subtraction of the combinatoric background.

The smooth background is modeled using the function

$$B(x) = P(x) \times \begin{cases} e^{c_1 x + c_2 x^2} & \text{for } x \le x_0 \\ e^{d_0 + d_1 x + d_2 x^2} & \text{for } x > x_0 \end{cases}, \qquad (1)$$

where $P(x) \equiv \frac{1}{2x}\sqrt{[x^2 - (m_D + m_\pi)^2][x^2 - (m_D - m_\pi)^2]}$ is a two-body phase-space factor and $x = M(D\pi)$. Only four parameters are free in the piecewise exponential: c_1, c_2, d_2, and x_0. The parameters d_0 and d_1 are fixed by requiring that $B(x)$ be continuous and differentiable at the transition point x_0. We account for the feeddown of peaking backgrounds by convolving Breit-Wigner (BW) functions [11] with a function describing the resolution and bias obtained from the simulation of these decays. The mass and width of the $D_1(2420)$ feeddown are fixed to the values obtained in the $D^{*+}\pi^-$ analysis described below, while the parameters of the $D_2^*(2460)$ feeddown are fixed to those of the true $D_2^*(2460)$ in the same $M(D\pi)$ distribution.

The $D_2^*(2460)$ is modeled using a relativistic BW function with the appropriate Blatt-Weisskopf centrifugal barrier factor [2]. The $D^*(2600)$ and $D^*(2760)$ are modeled with relativistic BW functions [2]. Finally, although not visible in the $M(D^+\pi^-)$ mass distribution, we include a BW function to account for the known resonance $D_0^*(2400)$, which is expected to decay to this final state. The χ^2 per number of degrees of freedom (NDF) of the fit decreases from 596/245 to 281/242 when this resonance is included. This resonance is very broad and is present together with the feeddown and $D_2^*(2460)^0$; therefore we restrict its mass and width parameters to be within 2σ of the known values [5]. The shapes of the signal components are corrected for a small variation of the efficiency as a function of $M(D\pi)$ and are multiplied by the two-body phase-space factor. They are also corrected for the mass resolution by convolving them with the resolution function determined from MC simulation of signal decays. The fit to the $M(D^+\pi^-)$ distribution (fit A) is shown in Fig. 2 (top). The results of this fit, as well as fits to the other final states described below, are shown in Table I. In this table, we show the significance for each new signal, defined as the signal yield divided by the total uncertainty on the yield.

The fit to the $D^0\pi^+$ mass spectrum is similar to that described for the $D^+\pi^-$ system. Because the feeddown is larger and the statistical precision of the resonances is not as good as for $D^+\pi^-$, we fix the width parameters of all resonances to the values determined from $D^+\pi^-$ assuming isospin symmetry. The fit to the $M(D^0\pi^+)$ mass distribution (fit B) is shown in Fig. 2 (bottom); this fit has χ^2/NDF of 278/224. We find consistent mass values for both $D^*(2600)$ and $D^*(2760)$ in the fits of the $D^+\pi^-$ and $D^0\pi^+$ mass distributions.

We now search for these new states in the $D^{*+}\pi^-$ decay mode. We define the variable $M(D^{*+}\pi^-) = m(K^-\pi^+(\pi^+\pi^-)\pi_s^+\pi^-) - m(K^-\pi^+(\pi^+\pi^-)\pi_s^+) + m_{D^{*+}}$ where $m_{D^{*+}}$ is the value of the D^{*+} mass [2]. The $D^{*+}\pi^-$ mass distribution is shown in Fig. 3 and shows the following features:

(i) Prominent $D_1(2420)^0$ and $D_2^*(2460)^0$ peaks.
(ii) Two additional enhancements at $\sim 2.60\ \mathrm{GeV}/c^2$ and $\sim 2.75\ \mathrm{GeV}/c^2$, which we initially denote as $D^*(2600)^0$ and $D(2750)^0$.

Studies of the generic MC simulation as well as studies of the D^{*+} sidebands and the wrong-sign sample ($D^{*+}\pi^+$) show no peaking backgrounds in this mass spectrum.

We fit $M(D^{*+}\pi^-)$ by parametrizing the background with the function in Eq. (1). The $D_1(2420)^0$ and $D_2^*(2460)^0$ resonances are modeled using relativistic BW functions with appropriate Blatt-Weisskopf form factors. The $D^*(2600)^0$ and $D(2750)^0$ are modeled with relativistic BW functions. The broad resonance $D_1'(2430)^0$ is known to decay to this final state, however, this fit is insensitive to it due to its large width (~ 380 MeV) [4] and because the background parameters are free.

TABLE I. Summary of the results. The first error is statistical and the second is systematic; "fixed" indicates the parameters were fixed to the values from fit A or C. The significance is defined as the yield divided by its total error.

Resonance	Channel (fit)	Efficiency (%)	Yield ($\times 10^3$)	Mass (MeV/c^2)	Width (MeV)	Significance
$D_1(2420)^0$	$D^{*+}\pi^-$ (C)		$102.8 \pm 1.3 \pm 2.3$	$2420.1 \pm 0.1 \pm 0.8$	$31.4 \pm 0.5 \pm 1.3$	
	$D^{*+}\pi^-$ (E)	1.09 ± 0.03	$214.6 \pm 1.2 \pm 6.4$	2420.1 (fixed)	31.4 (fixed)	
$D_2^*(2460)^0$	$D^+\pi^-$ (A)	1.29 ± 0.03	$242.8 \pm 1.8 \pm 3.4$	$2462.2 \pm 0.1 \pm 0.8$	$50.5 \pm 0.6 \pm 0.7$	
	$D^{*+}\pi^-$ (E)	1.12 ± 0.04	$136 \pm 2 \pm 13$	2462.2 (fixed)	50.5 (fixed)	
$D(2550)^0$	$D^{*+}\pi^-$(C)		$34.3 \pm 6.7 \pm 9.2$	$2539.4 \pm 4.5 \pm 6.8$	$130 \pm 12 \pm 13$	3.0σ
	$D^{*+}\pi^-$ (E)	1.14 ± 0.04	$98.4 \pm 8.2 \pm 38$	2539.4 (fixed)	130 (fixed)	
$D^*(2600)^0$	$D^+\pi^-$ (A)	1.35 ± 0.05	$26.0 \pm 1.4 \pm 6.6$	$2608.7 \pm 2.4 \pm 2.5$	$93 \pm 6 \pm 13$	3.9σ
	$D^{*+}\pi^-$ (D)		$50.2 \pm 3.0 \pm 6.7$	2608.7 (fixed)	93 (fixed)	7.3σ
	$D^{*+}\pi^-$ (E)	1.18 ± 0.05	$71.4 \pm 1.7 \pm 7.3$	2608.7 (fixed)	93 (fixed)	
$D(2750)^0$	$D^{*+}\pi^-$ (E)	1.23 ± 0.07	$23.5 \pm 2.1 \pm 5.2$	$2752.4 \pm 1.7 \pm 2.7$	$71 \pm 6 \pm 11$	4.2σ
$D^*(2760)^0$	$D^+\pi^-$ (A)	1.41 ± 0.09	$11.3 \pm 0.8 \pm 1.0$	$2763.3 \pm 2.3 \pm 2.3$	$60.9 \pm 5.1 \pm 3.6$	8.9σ
$D_2^*(2460)^+$	$D^0\pi^+$ (B)		$110.8 \pm 1.3 \pm 7.5$	$2465.4 \pm 0.2 \pm 1.1$	50.5 (fixed)	
$D^*(2600)^+$	$D^0\pi^+$ (B)		$13.0 \pm 1.3 \pm 4.5$	$2621.3 \pm 3.7 \pm 4.2$	93 (fixed)	2.8σ
$D^*(2760)^+$	$D^0\pi^+$ (B)		$5.7 \pm 0.7 \pm 1.5$	$2769.7 \pm 3.8 \pm 1.5$	60.9 (fixed)	3.5σ

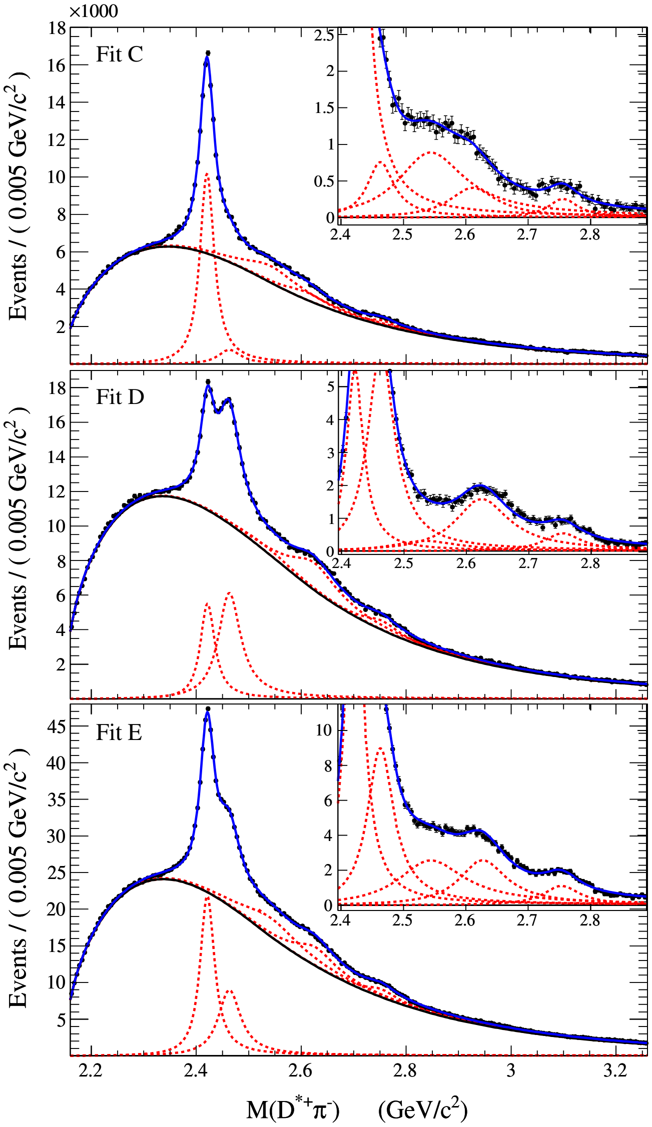

FIG. 3 (color online). Mass distributions for $D^{*+}\pi^-$ candidates. Top: candidates with $|\cos\theta_H| > 0.75$. Middle: candidates with $|\cos\theta_H| < 0.5$. Bottom: all candidates. Points correspond to data, with the total fit overlaid as a solid curve. The lower solid curve is the combinatoric background, and the dotted curves are the signal components. The inset plots show the distributions after subtraction of the combinatoric background.

Because of the vector nature of the D^{*+}, the $D^{*+}\pi^-$ final state contains additional information about the spin-parity (J^P) quantum numbers of the resonances. In the rest frame of the D^{*+}, we define the *helicity* angle θ_H as the angle between the primary pion π^- and the slow pion π^+ from the D^{*+} decay. The distributions in $\cos\theta_H$ for the predicted resonances, assuming parity conservation, are given in Table II. Initially, we have attempted to fit the $M(D^{*+}\pi^-)$ distribution incorporating only two new signals at $\sim$2.6 GeV/c^2 and at $\sim$2.75 GeV/c^2. However, when we extract the yields as a function of $\cos\theta_H$ we find that the mean value of the peak at $\sim$2.6 GeV/c^2 increases by $\sim$70 MeV/c^2 between $\cos\theta_H = -1$ and $\cos\theta_H = 0$, and decreases again as $\cos\theta_H \rightarrow +1$. This behavior suggests two resonances with different helicity-angle distributions are present in this mass region. To proceed we incorporate a new component, which we call $D(2550)^0$, into our model at $\sim$2.55 GeV/c^2. We extract the parameters of this component by requiring $|\cos\theta_H| > 0.75$ in order to suppress the other resonances. In this fit (fit C), shown in Fig. 3 (top), we fix the parameters of the $D_2^*(2460)^0$ and $D^*(2600)^0$ to those measured in $D^+\pi^-$. We obtain a χ^2/NDF of 214/205 for this fit. This fit also determines the parameters of the $D_1(2420)^0$. We then perform a complementary fit (fit D), shown in Fig. 3 (middle), in which we require $|\cos\theta_H| < 0.5$ to discriminate in favor of the $D^*(2600)^0$. We obtain a χ^2/NDF of 210/209 for this fit. To determine the final parameters of the $D(2750)^0$ signal we fit the total $D^{*+}\pi^-$ sample while fixing the parameters of all other BW components to the values determined in the previous fits. This final fit (fit E), shown in Fig. 3 (bottom), has a χ^2/NDF of 244/207.

TABLE II. Properties of the predicted states [1]. The value of the parameter h depends on the state.

State	Predicted mass	J^P	$\cos\theta_H$ distribution
$D_0^1(2S)$	2.58 GeV/c^2	0^-	$\propto \cos^2\theta_H$
$D_1^3(2S)$	2.64 GeV/c^2	1^-	$\propto \sin^2\theta_H$
$D_1^1(1P)$	2.44 GeV/c^2	1^+	$\propto 1 + h\cos^2\theta_H$
$D_0^3(1P)$	2.40 GeV/c^2	0^+	Decay not allowed
$D_1^3(1P)$	2.49 GeV/c^2	1^+	$\propto 1 + h\cos^2\theta_H$
$D_2^3(1P)$	2.50 GeV/c^2	2^+	$\propto \sin^2\theta_H$
$D_2^1(1D)$	$\sim$2.83 GeV/c^2	2^-	$\propto 1 + h\cos^2\theta_H$
$D_1^3(1D)$	2.82 GeV/c^2	1^-	$\propto \sin^2\theta_H$
$D_2^3(1D)$	$\sim$2.83 GeV/c^2	2^-	$\propto 1 + h\cos^2\theta_H$
$D_3^3(1D)$	2.83 GeV/c^2	3^-	$\propto \sin^2\theta_H$

Systematic uncertainties on all fit results are estimated by varying the parameters that were fixed in the fits and by varying the bin width and mass range of the histograms. In addition, the BW shape used for the new signals is replaced by that for a D-wave decay, and we vary the background model according to deviations observed when this model is used to fit the smooth distribution in the wrong-sign samples. A systematic uncertainty is also estimated from a possible contribution of the $D_1'(2430)$. Finally, we estimate uncertainties on the mass values due to uncertainties in the magnetic field and the SVT material density. Effects due to possible interference between the decay amplitudes for different excited states and the background amplitudes are ignored in this inclusive analysis.

The final model for the $M(D^{*+}\pi^-)$ distribution is used to extract the signal yields as a function of $\cos\theta_H$. We divide the data into 10 subsamples corresponding to $\cos\theta_H$ intervals of 0.2 between -1 and $+1$. Each sample is fitted with all shape parameters fixed to the values determined above. The yields extracted from these fits are plotted for each signal in Fig. 4. For the $D_1(2420)$ we measure the

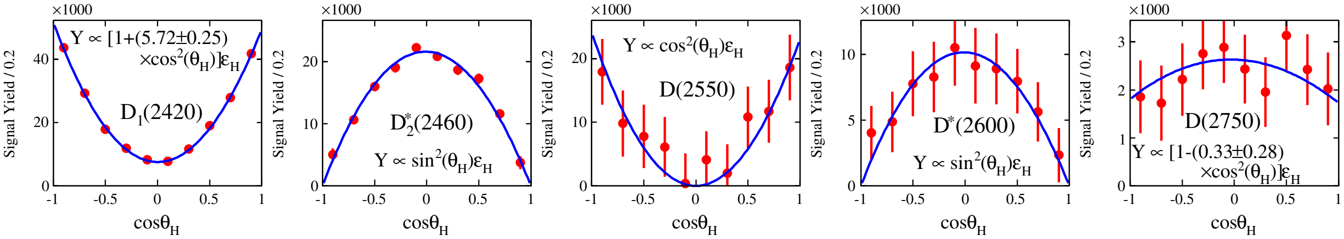

FIG. 4 (color online). Distribution in $\cos\theta_H$ for each signal in $D^{*+}\pi^-$. The error bars include statistical and correlated systematic uncertainties. The curve is a fit using the function Y shown in the plot; ε_H is the efficiency as a function of $\cos\theta_H$.

helicity parameter $h = 5.72 \pm 0.25$, where the error includes both statistical and systematic uncertainties. This value is consistent with the measurement by ZEUS [12]. The $\cos\theta_H$ distributions of the $D_2^*(2460)$ and $D^*(2600)$ are consistent with the expectations for *natural parity*, defined by $P = (-1)^J$, and leading to a $\sin^2\theta_H$ distribution. This observation supports the assumption that the enhancement assigned to the $D^*(2600)$ in the $D^+\pi^-$ and $D^{*+}\pi^-$ belong to the same state; only states with natural parity can decay to both $D^+\pi^-$ and $D^{*+}\pi^-$. The $\cos\theta_H$ distribution for the $D(2550)^0$ is consistent with pure $\cos^2\theta_H$ as expected for a $J^P = 0^-$ state.

The ratio of branching fractions $\frac{B(D^{**}\to D^+\pi^-)}{B(D^{**}\to D^{*+}\pi^-)}$ (where D^{**} labels any resonance) can be useful in the identification of the new signals with predicted states. We compute this ratio for the $D_2^*(2460)^0$, $D^*(2600)^0$, and $D(2750)^0$ using the yields obtained from the fits to the total samples and correcting for the reconstruction efficiency: $(N_{D\pi}/\varepsilon_{D\pi})/(N_{D^*\pi}/\varepsilon_{D^*\pi})$. The efficiencies and yields are shown in Table I. We find the following ratios:

$$\frac{B(D_2^*(2460)^0 \to D^+\pi^-)}{B(D_2^*(2460)^0 \to D^{*+}\pi^-)} = 1.47 \pm 0.03 \pm 0.16,$$

$$\frac{B(D^*(2600)^0 \to D^+\pi^-)}{B(D^*(2600)^0 \to D^{*+}\pi^-)} = 0.32 \pm 0.02 \pm 0.09,$$

$$\frac{B(D^*(2760)^0 \to D^+\pi^-)}{B(D(2750)^0 \to D^{*+}\pi^-)} = 0.42 \pm 0.05 \pm 0.11.$$

The first uncertainty is due to the statistical uncertainty on the yields. The second uncertainty includes the systematic uncertainty on the yields, the systematic uncertainty due to differences in PID and tracking efficiency, and the errors from the branching fractions for the decay chains [2]. Although in the last ratio the signal in the numerator may not be the same as the signal in the denominator, we determine the ratio, as it may help elucidate the nature of this structure.

In summary, we have analyzed the inclusive production of the $D^+\pi^-$, $D^0\pi^+$, and $D^{*+}\pi^-$ systems in search of new D-meson resonances using 454 fb^{-1} of data collected by the *BABAR* experiment. We observe for the first time four signals, which we denote $D(2550)^0$, $D^*(2600)^0$, $D(2750)^0$, and $D^*(2760)^0$. We also observe the isospin partners $D^*(2600)^+$ and $D^*(2760)^+$. The $D(2550)^0$ and $D^*(2600)^0$ have mass values and $\cos\theta_H$ distributions that are consistent with the predicted radial excitations $D_0^1(2S)$ and $D_1^3(2S)$. The $D^*(2760)^0$ signal observed in $D^+\pi^-$ is very close in mass to the $D(2750)^0$ signal observed in $D^{*+}\pi^-$; however, their mass and width values differ by 2.6σ and 1.5σ, respectively. Four $L = 2$ states are predicted to lie in this region [1], but only two are expected to decay to $D^+\pi^-$. This may explain the observed features.

We are grateful for the excellent luminosity and machine conditions provided by our PEP-II colleagues, and for the substantial dedicated effort from the computing organizations that support *BABAR*. The collaborating institutions wish to thank SLAC for its support and kind hospitality. This work is supported by DOE and NSF (USA), NSERC (Canada), CEA and CNRS-IN2P3 (France), BMBF and DFG (Germany), INFN (Italy), FOM (The Netherlands), NFR (Norway), MES (Russia), MICIIN (Spain), and STFC (United Kingdom). Individuals have received support from the Marie Curie EIF (European Union), the A. P. Sloan Foundation (USA), and the Binational Science Foundation (USA-Israel).

---

[1] S. Godfrey and N. Isgur, Phys. Rev. D **32**, 189 (1985).
[2] C. Amsler *et al.* (Particle Data Group), Phys. Lett. B **667**, 1 (2008).
[3] A. F. Falk and M. E. Peskin, Phys. Rev. D **49**, 3320 (1994).
[4] K. Abe *et al.* (Belle Collaboration), Phys. Rev. D **69**, 112002 (2004).
[5] B. Aubert *et al.* (*BABAR* Collaboration), Phys. Rev. D **79**, 112004 (2009).
[6] Charge conjugates are implied throughout this paper.

- [7] A. Abulencia *et al.* (CDF Collaboration), Phys. Rev. D **73**, 051104 (2006).
- [8] B. Aubert *et al.* (*BABAR* Collaboration), Nucl. Instrum. Methods Phys. Res., Sect. A **479**, 1 (2002).
- [9] T. Sjöstrand, Comput. Phys. Commun. **82**, 74 (1994).
- [10] S. Agostinelli *et al.* (GEANT4 Collaboration), Nucl. Instrum. Methods Phys. Res., Sect. A **506**, 250 (2003).
- [11] G. Breit and E. Wigner, Phys. Rev. **49**, 519 (1936).
- [12] S. Chekanov *et al.* (ZEUS Collaboration), Eur. Phys. J. C **60**, 25 (2009).